Asociación Argentina
de Mecánica Computacional

Mecánica Computacional Vol XXV, pp. 2747-2768
Alberto Cardona, Norberto Nigro, Victorio Sonzogni, Mario Storti. (Eds.)
Santa Fe, Argentina, Noviembre 2006

A BOUNDARY ELEMENT FORMULATION FOR MODELING MICRO-HETEROGENEOUS MATERIALS

Federico C. Buroni[a] **and Rogério J. Marczak**[b]

[a] *Mechanical Engineering Department, Universidade Federal do Rio Grande do Sul, Rua Sarmento Leite 425, 90050-170, Porto Alegre 3492, RS, Brazil*
fedeburoni@yahoo.com.br

[b] *Mechanical EngineeringDepartment, Universidade Federal do Rio Grande do Sul, Rua Sarmento Leite 425, 90050-170, Porto Alegre 3492, RS, Brazil*
rato@mecanica.ufrgs.br

Keywords: Micro-heterogeneous materials, composite, microstructure modeling, boundary element method, hole element, inclusion element.

Abstract. This work presents a Boundary Element Method formulation for modeling two-dimensional microstructures containing cylindrical voids and inclusions. Inhomogeneities are modeled in an efficient way by using a single specially developed element. Trigonometric functions are used as a base for the element shape functions. A static condensation scheme is performed on the system of equations to further improve the efficiency of the formulation. The accuracy of the proposed method is illustrated with some examples.

1 INTRODUCTION

Industrial materials, like everything in Nature, are heterogeneous when observed at a certain scale. The determination of the macroscopic characteristics of heterogeneous materials is an essential problem in many applications of engineering and science. The study of relationships between microstructural phenomenon and the macroscopic behavior not only allows predicting the behavior of existing materials, but also provides a tool for the design of new micro-structures, in such a way that the resulting macroscopic behavior agrees with desired characteristics.

Currently, the use of numerical methods to solve differential equations such as the Finite Element Method (FEM), the Boundary Element Method (BEM), or the Finite Difference Method is fully generalized. The combination of micro-mechanics and such numerical methods supplies a powerful tool for materials behavior modeling. The BEM has already shown to be more accurate and efficient in terms of computational cost than other popular methods for many linear problems in Solids Mechanics, for a given accuracy level. Particularly in overall properties predictions, the BEM can make more efficient predictions (Yang & Qin, 2004) because the spatial average scheme of the internal fields of the variables requires only information of the micro-structure boundary. In this work, the BEM is used to solve the elastic problem in a microstructured material. The main goal is to develop an efficient Boundary Element Formulation for modeling composite materials with random distributions of inhomogeneities.

In this paper the material is considered as an isotropic and homogeneous matrix containing cylindrical voids and inclusions. In order to reduce both, the amount of data and computational cost the problem is considered 2D with circular cylindrical holes and inclusions perpendicular to the model plane. Thus, the formulations of Henry & Banerjee, 1991 for modeling three-dimensional elastic solids containing tubular holes and of Banerjee & Henry, 1992 for fiber inclusions are particularized to two-dimensions and presented in a general way. Each void or inclusion is modeled with a single, specially developed *hole element* or *inclusion element*, respectively. Thus, the microstructure discretization strategy becomes simply the indication of the center of each inhomogeneity, its radius and the element order, in addition to the conventional outer boundary element mesh. Trigonometric functions are proposed as a base for the element shape functions resulting in elements with 4, 5 and 6 nodes in addition to original 3-node element proposed by Henry & Banerjee (1991). The integration of strongly singular kernels found in the hole/inclusion element is accomplished by the direct method, resulting a regularized element. A static condensation scheme is performed on the system of equations to further improve the performance of the formulation. The accuracy of the proposed method is illustrated by some examples of microstructure materials containing voids.

2 BOUNDARY ELEMENT FORMULATION

2.1 Boundary integral equation for a matrix with cylindrical voids

The direct boundary integral equation for displacements (Banerjee, 1994) of an elastic solid can be applied to solve the Boundary Value Problem (BVP) of a microstructure with

domain Ω surrounded by an exterior boundary Γ_o containing cylindrical micro-voids with boundary Γ. In absence of body force this equation is expressed as (Henry & Banerjee, 1991):

$$\mathbf{C}_{ij}(\xi)u_i(\xi) = \int_{\Gamma_o}\left[G_{ij}^o(x,\xi)t_i^o(x) - F_{ij}^o(x,\xi)u_i^o(x)\right]d\Gamma + \\ + \sum_{n=1}^{N_f}\int_{\Gamma^n}\left[G_{ij}^f(x,\xi)t_i^f(x) - F_{ij}^f(x,\xi)u_i^f(x)\right]d\Gamma \tag{1}$$

where u_i and t_i are the Cartesian components of the boundary displacements and tractions, G_{ij} and F_{ij} are the Kelvin fundamental solution at a point ξ due to the unit load placed at location x, $\mathbf{C}_{ij}(\xi)$ is a function of boundary geometry at the point ξ, and N_f is the number of voids. The superscripts *o* and *f* (no sum) refer to the quantities on the outer boundary of the matrix and on the boundary of the voids, respectively. Contrary to the conventional discretization of the equation (1), which requires fine meshing for each void, the present approach allows an efficient analysis, significantly reducing the input data amount and the number of degrees of freedom.

A local coordinate system $\hat{x}_i$ is defined with its origin coincident with the hole center. The symbol $(\hat{\cdot})$ is used to refer the variables in the local system. The local system origin in the global co-ordinate system x_i is determined by the vectors z_i, while the axis $\hat{x}_i$ are kept parallel to x_i as is indicated in Fig. 1.

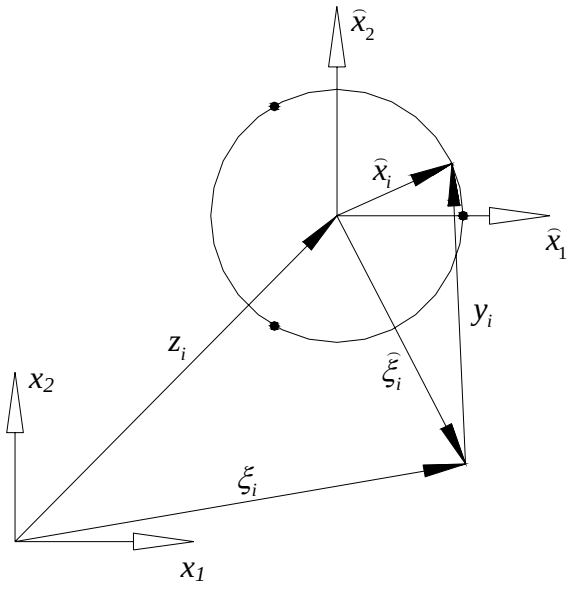

Figure 1: Local and global reference system.

Thus, a particular hole boundary point $\hat{x}_i$ can be expressed as function of angle θ according to:

$$\begin{aligned} \hat{x}_1 &= R\cos\theta \\ \hat{x}_2 &= R\,\mathrm{sen}\,\theta \end{aligned} \tag{2}$$

where R is the radius of the hole. The normal vectors at $\hat{x}_i$ are expressed by:

$$\begin{aligned} \hat{n}_1 &= -\cos\theta \\ \hat{n}_2 &= -\mathrm{sen}\,\theta \end{aligned} \tag{3}$$

Considering the case which no internal pressure is applied in the hole, the first integral in the sum of the RHS of equation (1) vanishes. The second term can be mapped to the local system and integrated in the circumferential direction as in Henry & Banerjee (1991). For the n-th hole one has:

$$\int_{\Gamma^n} F_{ij}^f\left(x,\xi\right)u_i^f\left(x\right)d\Gamma = \int_{2\pi}^{0} \hat{F}_{ij}^f\left(R,\theta,\bar{\xi}\right)u_i^f\left(\theta\right)Rd\theta \tag{4}$$

In this work, the analytic expressions of the tensor $\hat{F}_{ij}$ are developed for the reference system $\hat{x}_i$, resulting in the following expressions, valid for *plane stress* and *plane strain* states:

$$\hat{F}_{11}\left(R,\theta,\bar{\xi}\right) = \left[\frac{C_3}{r^2\left(R,\theta,\bar{\xi}\right)}\right]\left\{\left[C_4 + \frac{2\left(R\cos\theta-\bar{\xi}_1\right)^2}{r^2\left(R,\theta,\bar{\xi}\right)}\right]\left[\bar{\xi}_1\cos\theta+\bar{\xi}_2\,\mathrm{sen}\,\theta-R\right]\right\} \tag{5}$$

$$\begin{aligned} &\hat{F}_{21}\left(R,\theta,\bar{\xi}\right) = \\ &= \left[\frac{C_3}{r^2\left(R,\theta,\bar{\xi}\right)}\right]\left\{C_4\left[\bar{\xi}_1\,\mathrm{sen}\,\theta-\bar{\xi}_2\cos\theta\right] + \left[\frac{2\left(R\cos\theta-\bar{\xi}_1\right)\left(R\,\mathrm{sen}\,\theta-\bar{\xi}_2\right)}{r^2\left(R,\theta,\bar{\xi}\right)}\right]\left[\bar{\xi}_1\cos\theta+\bar{\xi}_2\,\mathrm{sen}\,\theta-R\right]\right\} \end{aligned} \tag{6}$$

$$\begin{aligned} &\hat{F}_{12}\left(R,\theta,\bar{\xi}\right) = \\ &= \left[\frac{C_3}{r^2\left(R,\theta,\bar{\xi}\right)}\right]\left\{C_4\left[\bar{\xi}_2\cos\theta-\bar{\xi}_1\,\mathrm{sen}\,\theta\right] + \left[\frac{2\left(R\cos\theta-\bar{\xi}_1\right)\left(R\,\mathrm{sen}\,\theta-\bar{\xi}_2\right)}{r^2\left(R,\theta,\bar{\xi}\right)}\right]\left[\bar{\xi}_1\cos\theta+\bar{\xi}_2\,\mathrm{sen}\,\theta-R\right]\right\} \end{aligned} \tag{7}$$

$$\hat{F}_{22}\left(R,\theta,\bar{\xi}\right) = \left[\frac{C_3}{r^2\left(R,\theta,\bar{\xi}\right)}\right]\left\{\left[C_4 + \frac{2\left(R\,\mathrm{sen}\,\theta-\bar{\xi}_2\right)^2}{r^2\left(R,\theta,\bar{\xi}\right)}\right]\left[\bar{\xi}_1\cos\theta+\bar{\xi}_2\,\mathrm{sen}\,\theta-R\right]\right\} \tag{8}$$

where the constants C_3 and C_4 are:

$$\begin{aligned} C_3 &= \frac{1}{4\pi\left(1-\nu\right)} \\ C_4 &= 1-2\nu \end{aligned} \tag{9}$$

and ν is the Poisson's ratio. The variable r is then defined as:

$$r^2\left(R,\theta,\bar{\xi}\right) = \left(R\cos\theta-\bar{\xi}_1\right)^2 + \left(R\,\mathrm{sen}\,\theta-\bar{\xi}_2\right)^2 \tag{10}$$

The above expressions are particularized for plane strain hypothesis. For the plane stress case, ν is replaced by $\bar{\nu} = \nu/(1+\nu)$.

Finally, the boundary integral equation for the problem of a matrix containing N_f cylindrical holes without internal pressure is given by:

$$\mathbf{C}_{ij}(\xi)u_i(\xi) = \int_{\Gamma_o}\left[G_{ij}^o(x,\xi)t_i^o(x) - F_{ij}^o(x,\xi)u_i^o(x)\right]d\Gamma - \\ -\sum_{n=1}^{N_f}\int_{2\pi}^{0}\widehat{F}_{ij}^f\left(R,\theta,\widehat{\xi}\right)u_i^f(\theta)R_n d\theta \tag{11}$$

2.2 Boundary integral equation for a matrix with cylindrical inclusions

In cases where the inhomogeneity in the material matrix is an inclusion of another material, the boundary integral equation for displacements remains the same presented for a matrix with voids (see equation (11)), and N_f is replaced by the number of inclusions N_p. The boundary integral equation for each inclusion can be written as (Banerjee & Henry, 1992):

$$\mathbf{C}_{ij}^p(\xi)u_i(\xi) = \int_{\Gamma^n}\left[G_{ij}^p(x,\xi)t_i^p(x) - F_{ij}^p(x,\xi)u_i^p(x)\right]d\Gamma \tag{12}$$

where *p* denotes current inclusion. If a perfect bonding between the inclusion and the matrix is assumed, the displacements and tractions of the matrix boundary are related to those of the inclusion boundary by compatibility conditions:

$$u_i^f(x) = u_i^p(x), \quad t_i^f(x) = -t_i^p(x) \tag{13}$$

Substitution of equation (13) into equation (12) yields the following modified boundary integral equation for the *n*-th inclusion:

$$\mathbf{C}_{ij}^p(\xi)u_i(\xi) = \int_{\Gamma^n}\left[-G_{ij}^p(x,\xi)t_i^f(x) - F_{ij}^p(x,\xi)u_i^f(x)\right]d\Gamma \tag{14}$$

Adding the N_p inclusion (equations (14)) to the boundary integral equation of the matrix results the modified boundary integral equation for the composite matrix:

$$\mathbf{C}_{ij}^{\Theta}(\xi)u_i(\xi) = \int_{\Gamma_o}\left[G_{ij}^o(x,\xi)t_i^o(x) - F_{ij}^o(x,\xi)u_i^o(x)\right]d\Gamma + \\ +\sum_{n=1}^{N_p}\int_{\Gamma^n}\left[G_{ij}^{\Theta}(x,\xi)t_i^f(x) - F_{ij}^{\Theta}(x,\xi)u_i^f(x)\right]d\Gamma \tag{15}$$

where

$$G_{ij}^{\Theta}(x,\xi) = G_{ij}^f(x,\xi) - G_{ij}^p(x,\xi) \tag{16}$$

$$F_{ij}^{\Theta}(x,\xi) = F_{ij}^f(x,\xi) + F_{ij}^p(x,\xi) \tag{17}$$

Note that G_{ij}^f and G_{ij}^p have similar expressions. However, the material constants in G_{ij}^f refer to the matrix while the properties of each inclusion are considered in G_{ij}^p. The same happens with the F_{ij} tensor. The signs of F_{ij}^f and F_{ij}^p are opposites taking into account the external normal to the boundary. In the formulation of Banerjee & Henry (1992) the F_{ij}^{Θ} tensor is null under the argument that the Poisson's ratio of the matrix and the inclusion are equal when the Young's modulus of the inclusion is much greater than the modulus of the matrix. In the present work, this assumption is relaxed, posing no restrictions to the Poisson's ratios

between matrix and inclusion.

The integral terms in the sum of the RHS in equation (15) can be mapped to the local system and integrated in the circumferential direction. Therefore, for *n*-th inclusion:

$$\int_{\Gamma^n} F_{ij}^{\Theta}(x,\xi)u_i^f(x)d\Gamma = \int_{2\pi}^{0} \widehat{F}_{ij}^{\Theta}\left(R,\theta,\bar{\xi}\right)u_i^f(\theta)Rd\theta \tag{18}$$

$$\int_{\Gamma^n} G_{ij}^{\Theta}(x,\xi)t_i^f(x)d\Gamma = \int_{2\pi}^{0} \widehat{G}_{ij}^{\Theta}\left(R,\theta,\bar{\xi}\right)t_i^f(\theta)Rd\theta \tag{19}$$

In this work, the analytic expressions of the tensor $\widehat{G}_{ij}$ are developed for the local system $\widehat{x}_i$, resulting in the following expressions, valid for both *plane stress* and *plane strain*:

$$\widehat{G}_{11}\left(R,\theta,\bar{\xi}\right) = C_1\left[C_2\ln\left(\sqrt{r^2\left(R,\theta,\bar{\xi}\right)}\right) - \frac{\left(R\cos\theta-\bar{\xi}_1\right)^2}{r^2\left(R,\theta,\bar{\xi}\right)}\right] \tag{20}$$

$$\widehat{G}_{21}\left(R,\theta,\bar{\xi}\right) = C_1\left[\frac{\left(R\cos\theta-\bar{\xi}_1\right)\left(R\,\mathrm{sen}\,\theta-\bar{\xi}_2\right)}{r^2\left(R,\theta,\bar{\xi}\right)}\right] \tag{21}$$

$$\widehat{G}_{22}\left(R,\theta,\bar{\xi}\right) = C_1\left[C_2\ln\left(\sqrt{r^2\left(R,\theta,\bar{\xi}\right)}\right) - \frac{\left(R\,\mathrm{sen}\,\theta-\bar{\xi}_2\right)^2}{r^2\left(R,\theta,\bar{\xi}\right)}\right] \tag{22}$$

$$\widehat{G}_{12}\left(R,\theta,\bar{\xi}\right) = C_1\left[\frac{\left(R\cos\theta-\bar{\xi}_1\right)\left(R\,\mathrm{sen}\,\theta-\bar{\xi}_2\right)}{r^2\left(R,\theta,\bar{\xi}\right)}\right] \tag{23}$$

and the constants C_1 and C_2 are:

$$C_1 = -\frac{1}{8\pi\mu(1-\nu)} \tag{24}$$

$$C_2 = 3-4\nu \tag{25}$$

Finally, boundary integral equation for the composite matrix with N_p inclusions is written:

$$\begin{aligned}\mathbf{C}_{ij}^{\Theta}(\xi)u_i(\xi) = &\int_{\Gamma_o}\left[G_{ij}^o(x,\xi)t_i^o(x) - F_{ij}^o(x,\xi)u_i^o(x)\right]d\Gamma + \\ &+\sum_{n=1}^{N_p}\int_{2\pi}^{0}\left[\widehat{G}_{ij}^{\Theta}\left(R,\theta,\bar{\xi}\right)t_i^f(\theta) - \widehat{F}_{ij}^{\Theta}\left(R,\theta,\bar{\xi}\right)u_i^f(\theta)\right]Rd\theta\end{aligned} \tag{26}$$

2.3 Discretization of the integral equation

In order to solve numerically the equations (11) and (26) the boundary is discretized in boundary elements whose displacements and tractions are interpolated from their nodal values. Writing the discretized form of the boundary integral equation for each nodal point results in a linear algebraic system of equations. After the application of the boundary conditions, this system can be solved and provided an approximate solution for the unknowns

on the boundary (Brebbia & Dominguez, 1992).

The displacement and traction fields on the boundary of the inhomogeneity are interpolated with special shape functions M_i:

$$u_i = M_\beta U_i^\beta \tag{27}$$

$$t_i = M_\beta T_i^\beta \tag{28}$$

where U_i^β and T_i^β are the displacements and tractions of the node β in the direction *i* and β ranges from 1 to the number of nodes of the element. The M_i functions are trigonometric circular functions with unitary value on the *n*-th node and zero on the others. These functions are used to interpolate both geometry and physical variables. The present formulation allows for the use of hole/inclusion elements with 3, 4, 5 and 6 nodes. The 3-node element employs the same functions proposed by Henry & Banerjee (1991):

$$\begin{aligned} M_1(\theta) &= \frac{1}{3} + \frac{2}{3}\cos\theta \\ M_2(\theta) &= \frac{1}{3} + \frac{\sqrt{3}}{3}\operatorname{sen}\theta - \frac{1}{3}\cos\theta \\ M_3(\theta) &= \frac{1}{3} - \frac{\sqrt{3}}{3}\operatorname{sen}\theta - \frac{1}{3}\cos\theta \end{aligned} \tag{29}$$

The shape functions of the higher order elements proposed herein are given by:

$$\begin{aligned} M_1(\theta) &= \frac{(1+\cos\theta)}{2}\cos\theta \\ M_2(\theta) &= \frac{1}{2} + \frac{1}{2}\operatorname{sen}\theta - \frac{1}{2}\cos^2\theta \\ M_3(\theta) &= \frac{(-1+\cos\theta)}{2}\cos\theta \\ M_4(\theta) &= \frac{1}{2} - \frac{1}{2}\operatorname{sen}\theta - \frac{1}{2}\cos^2\theta \end{aligned} \tag{30}$$

for the 4-node element,

$$\begin{aligned} M_1(\theta) &= -\frac{1}{5} + \frac{2}{5}\cos\theta + \frac{4}{5}\cos^2\theta \\ M_2(\theta) &= \frac{342}{899}\operatorname{sen}\theta + \frac{845}{1797}\operatorname{sen}\theta\cos\theta + \frac{122}{987}\cos\theta - \frac{2706}{4181}\cos^2\theta + \frac{10946}{20905} \\ M_3(\theta) &= \frac{845}{3594}\operatorname{sen}\theta - \frac{684}{899}\operatorname{sen}\theta\cos\theta - \frac{1353}{4181}\cos\theta + \frac{244}{987}\cos^2\theta + \frac{377}{4935} \\ M_4(\theta) &= -\frac{845}{3594}\operatorname{sen}\theta + \frac{684}{899}\operatorname{sen}\theta\cos\theta - \frac{1353}{4181}\cos\theta + \frac{244}{987}\cos^2\theta + \frac{377}{4935} \\ M_5(\theta) &= -\frac{342}{899}\operatorname{sen}\theta - \frac{845}{1797}\operatorname{sen}\theta\cos\theta + \frac{122}{987}\cos\theta - \frac{2706}{4181}\cos^2\theta + \frac{10946}{20905} \end{aligned} \tag{31}$$

for the 5-node element, and

$$
\begin{aligned}
M_1(\theta) &= -\frac{1}{6} - \frac{1}{6}\cos\theta + \frac{2}{3}\cos^2\theta + \frac{2}{3}\cos^3\theta \\
M_2(\theta) &= \frac{390}{1351}\operatorname{sen}\theta + \frac{780}{1351}\operatorname{sen}\theta\cos\theta - \frac{1}{3}\cos^2\theta - \frac{2}{3}\cos^3\theta + \frac{2}{3}\cos\theta + \frac{1}{3} \\
M_3(\theta) &= \frac{390}{1351}\operatorname{sen}\theta - \frac{780}{1351}\operatorname{sen}\theta\cos\theta - \frac{2}{3}\cos\theta - \frac{1}{3}\cos^2\theta + \frac{2}{3}\cos^3\theta + \frac{1}{3} \\
M_4(\theta) &= -\frac{1}{6} + \frac{1}{6}\cos\theta + \frac{2}{3}\cos^2\theta - \frac{2}{3}\cos^3\theta \\
M_5(\theta) &= -\frac{390}{1351}\operatorname{sen}\theta + \frac{780}{1351}\operatorname{sen}\theta\cos\theta - \frac{2}{3}\cos\theta - \frac{1}{3}\cos^2\theta + \frac{2}{3}\cos^3\theta + \frac{1}{3} \\
M_6(\theta) &= -\frac{390}{1351}\operatorname{sen}\theta - \frac{780}{1351}\operatorname{sen}\theta\cos\theta + \frac{2}{3}\cos\theta - \frac{1}{3}\cos^2\theta - \frac{2}{3}\cos^3\theta + \frac{1}{3}
\end{aligned}
\tag{32}
$$

for the 6-node element. The shape functions given by equations (29)-(32), are plotted in Figs. 2-5, respectively.

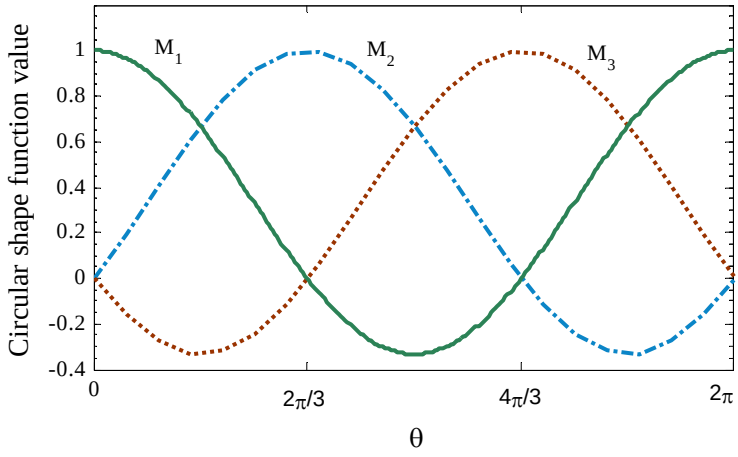

Figure 2: Circular shape functions used in the 3-node hole/inclusion element.

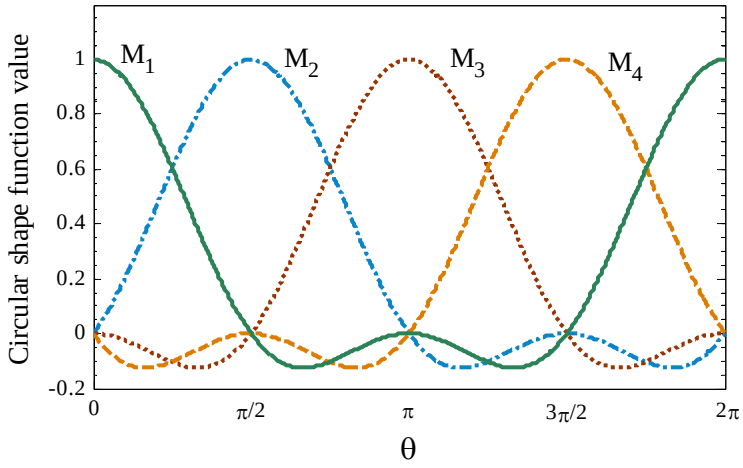

Figure 3: Circular shape functions used in the 4-node hole/inclusion element.

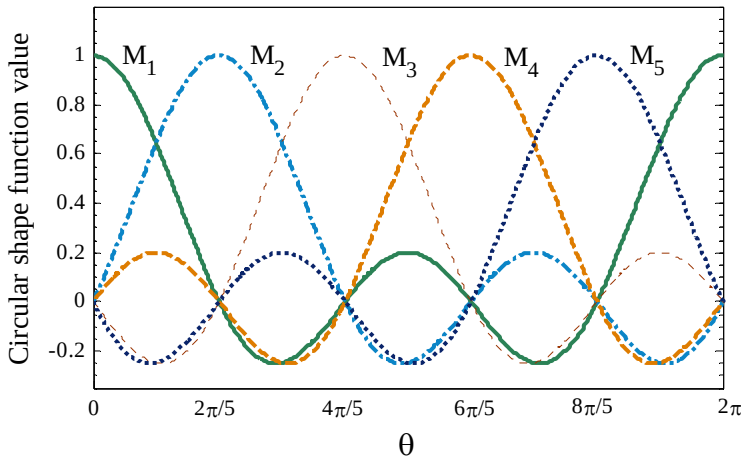

Figure 4: Circular shape functions used in the 3-node hole/inclusion element.

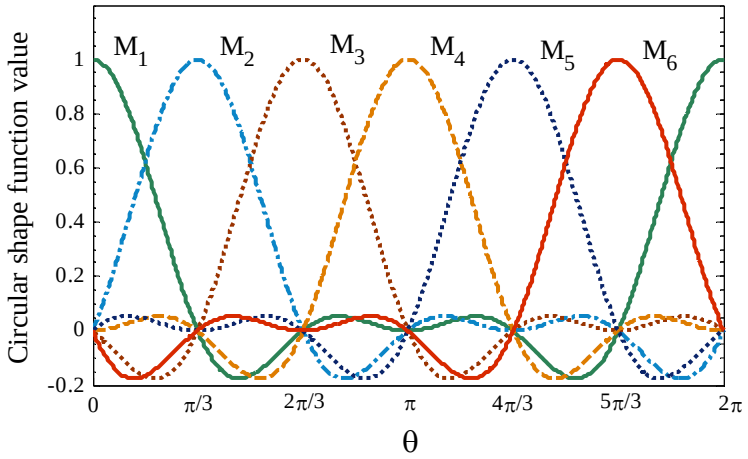

Figure 5: Circular shape functions used in the 3-node hole/inclusion element.

The numerical implementation of the formulation employs discontinuous quadratic elements (Brebbia & Dominguez, 1992) to discretize the outer boundary of the microstructure Γ_o. The modified shape functions matrix for a discontinuous quadratic element is found to be:

$$[\mathbf{\Phi}][\mathbf{Q}] = \begin{bmatrix} \bar{\phi}_1 & 0 & \bar{\phi}_2 & 0 & \bar{\phi}_3 & 0 \\ 0 & \bar{\phi}_1 & 0 & \bar{\phi}_2 & 0 & \bar{\phi}_3 \end{bmatrix} \tag{33}$$

where

$$\bar{\phi}_1 = \frac{\eta(\eta - 1 + b)}{2 + a^2 + ab - 3a}$$
$$\bar{\phi}_2 = \frac{\eta(a - b - \eta) - a + ab + 1 - b}{-a + ab + 1 - b} \tag{34}$$
$$\bar{\phi}_3 = \frac{-\eta(a - 1 - \eta)}{2 + b^2 + ab - 3b}$$

and $\eta = [-1;+1]$ is the normalized co-ordinate. The variables a and b are the left and right node offsets, respectively, as indicated in Fig. 6. The geometry is interpolated with the Lagrangean shape functions $[\mathbf{\Phi}]$, while the physical variables are interpolated with the modified shape functions of Eq. (34).

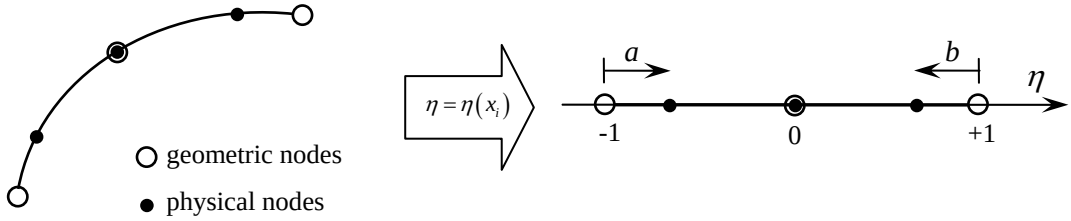

Figure 6: Mapping of discontinuous quadratic element to the normalized space η.

The displacement $\mathbf{u} = \lfloor u_1 \quad u_2 \rfloor^T$ and the tractions $\mathbf{t} = \lfloor t_1 \quad t_2 \rfloor^T$ fields are interpolated, for the outer material matrix elements, respectively by:

$$\{\mathbf{u}\} = [\mathbf{\Phi}][\mathbf{Q}]\{\mathbf{U}\} \tag{35}$$

$$\{\mathbf{t}\} = [\mathbf{\Phi}][\mathbf{Q}]\{\mathbf{T}\} \tag{36}$$

and for the hole or inclusion elements by:

$$\{\mathbf{u}\} = [\mathbf{M}]\{\mathbf{U}\} \tag{37}$$

$$\{\mathbf{t}\} = [\mathbf{M}]\{\mathbf{T}\} \tag{38}$$

where the displacements and tractions nodal vectors are given by:

$$\{\mathbf{U}\} = \lfloor U_1^1 \quad U_2^1 \quad U_1^2 \quad U_2^2 \quad U_1^3 \quad U_2^3 \rfloor^T \tag{39}$$

$$\{\mathbf{T}\} = \lfloor T_1^1 \quad T_2^1 \quad T_1^2 \quad T_2^2 \quad T_1^3 \quad T_2^3 \rfloor^T \tag{40}$$

for the discontinuous quadratic elements and:

$$\{\mathbf{U}\} = \lfloor U_1^1 \quad U_2^1 \quad U_1^2 \quad U_2^2 \quad \ldots \quad \ldots \quad U_1^{nn} \quad U_2^{nn} \rfloor^T \tag{41}$$

$$\{\mathbf{T}\} = \begin{bmatrix} T_1^1 & T_2^1 & T_1^2 & T_2^2 & \dots & \dots & T_1^{nn} & T_2^{nn} \end{bmatrix}^T \tag{42}$$

for the hole or inclusion elements. In equations (41)-(42), *nn* is the number of nodes used in the element. The shape functions matrix for the hole/inclusion element area arranged accordingly their number of nodes, using equations (29)-(32):

$$\mathbf{M} = \begin{bmatrix} M_1 & 0 & M_2 & 0 & \dots & \dots & M_{nn} & 0 \\ 0 & M_1 & 0 & M_2 & \dots & \dots & 0 & M_{nn} \end{bmatrix} \tag{43}$$

The boundary integral equation for the domain of the material matrix containing free stress cylindrical holes (see equation (11)) and inclusions (see equation (26)) is:

$$\begin{aligned} \mathbf{C}_{ij}(\xi) u_i(\xi) = & \int_{\Gamma_o} \left[G_{ij}^o(x,\xi) t_i^o(x) - F_{ij}^o(x,\xi) u_i^o(x) \right] d\Gamma - \\ & - \sum_{n=1}^{N_f} \int_{2\pi}^0 \widehat{F}_{ij}^f \left(R,\theta,\bar{\xi} \right) u_i^f(\theta) R_n d\theta + \\ & + \sum_{n=1}^{N_p} \int_{2\pi}^0 \left[\widehat{G}_{ij}^{\Theta} \left(R,\theta,\bar{\xi} \right) t_i^f(\theta) - \widehat{F}_{ij}^{\Theta} \left(R,\theta,\bar{\xi} \right) u_i^f(\theta) \right] R_n d\theta \end{aligned} \tag{44}$$

Using the corresponding shape functions to interpolate the displacements and tractions fields for each case, equation (44) can be written in the discretized form as:

$$\begin{aligned} [\mathbf{C}]^i \{\mathbf{U}\}^i = & \sum_{j=1}^{NE} \left[\int_{\Gamma_j} \left[\mathbf{G}^o \right]^T [\mathbf{\Phi}][\mathbf{Q}] d\Gamma \{\mathbf{T}\}^j \right] - \sum_{j=1}^{NE} \left[\int_{\Gamma_j} \left[\mathbf{F}^o \right]^T [\mathbf{\Phi}][\mathbf{Q}] d\Gamma \{\mathbf{U}\}^j \right] - \\ & - \sum_{n=1}^{N_f} \left[\int_{2\pi}^0 \left[\mathbf{F}^f \right]^T [\mathbf{M}] R_n d\theta \{\mathbf{U}\}^n \right] + \\ & + \sum_{n=1}^{N_p} \left[\int_{2\pi}^0 \left[\mathbf{G}^{\Theta} \right]^T [\mathbf{M}] R_n d\theta \{\mathbf{T}\}^n \right] - \sum_{n=1}^{N_p} \left[\int_{2\pi}^0 \left[\mathbf{F}^{\Theta} \right]^T [\mathbf{M}] R_n d\theta \{\mathbf{U}\}^n \right] \end{aligned} \tag{45}$$

where *NE* is the number of elements used to discretize the outer boundary of the material matrix Γ_o, N_f is the number of holes and N_p is the number of inclusions in the microstructure. Thus, equation (45) is the discretized form of the boundary integral equation for collocation point on node *i*. The column vector $\{\mathbf{U}\}^j$ and $\{\mathbf{T}\}^j$ are the displacements and tractions of element *j* (see equations (39)-(42)). The equation (45) can be rewritten, for each collocation point *i*:

$$\begin{aligned} [\mathbf{C}]^i \{\mathbf{U}\}^i = & \sum_{j=1}^{NNO} \left[\int_{\Gamma_j} \left[\mathbf{G}^o \right]^T \left[\bar{\mathbf{\Phi}}_q \right] d\Gamma \{\mathbf{T}\}^j \right] - \sum_{j=1}^{NNO} \left[\int_{\Gamma_j} \left[\mathbf{F}^o \right]^T \left[\bar{\mathbf{\Phi}}_q \right] d\Gamma \{\mathbf{U}\}^j \right] - \\ & - \sum_{n=1}^{NNF} \left[\int_{2\pi}^0 \left[\mathbf{F}^f \right]^T \left[\mathbf{M}_q \right] R_n d\theta \{\mathbf{U}\}^n \right] + \\ & + \sum_{n=1}^{NNP} \left[\int_{2\pi}^0 \left[G^{\Theta} \right]^T \left[\mathbf{M}_q \right] R_n d\theta \{\mathbf{T}\}^n \right] - \sum_{n=1}^{NNP} \left[\int_{2\pi}^0 \left[\mathbf{F}^{\Theta} \right]^T \left[\mathbf{M}_q \right] R_n d\theta \{\mathbf{U}\}^n \right] \end{aligned} \tag{46}$$

where *NNO* is the number of nodes of the outer boundary of material matrix, *NNF* is the number of nodes for the holes elements and *NNP* is the number of nodes for the inclusion elements in the microstructure. In this expression, the column vector $\{\mathbf{U}\}^j$ and $\{\mathbf{T}\}^j$ are the

displacements and tractions in the node j. The definition $\left[\bar{\mathbf{\Phi}}\right]=\left[\mathbf{\Phi}\right]\left[\mathbf{Q}\right]$ is used to interpolate the physical unknown in the discontinuous quadratic elements and the subscript q (q=1..3) point out the order of node j within the respective element. The equation (46) is written in a more compact form:

$$\sum_{j=1}^{NNO}\left[\left[\mathbf{F}\bar{\mathbf{\Phi}}\right]^{ij}\left\{\mathbf{U}\right\}^{j}\right]+\sum_{n=1}^{NNF}\left[\left[\mathbf{F}^{f}\mathbf{M}\right]^{in}\left\{\mathbf{U}\right\}^{n}\right]+\sum_{n=1}^{NNP}\left[\left[\mathbf{F}^{\Theta}\mathbf{M}\right]^{in}\left\{\mathbf{U}\right\}^{n}\right]=\sum_{j=1}^{NNO}\left[\left[\mathbf{G}\bar{\mathbf{\Phi}}\right]^{ij}\left\{\mathbf{T}\right\}^{j}\right]+ +\sum_{n=1}^{NNP}\left[\left[\mathbf{G}^{\Theta}\mathbf{M}\right]^{in}\left\{\mathbf{T}\right\}^{n}\right] \tag{47}$$

with the following definitions:

$$\left[\mathbf{G}\bar{\mathbf{\Phi}}\right]^{ij}=\int_{\Gamma_j}\begin{bmatrix}G_{11}^{ij} & G_{12}^{ij}\\ G_{21}^{ij} & G_{22}^{ij}\end{bmatrix}_{o}^{T}\begin{bmatrix}\bar{\phi}_q & 0\\ 0 & \bar{\phi}_q\end{bmatrix}d\Gamma \tag{48}$$

$$\left[\mathbf{F}\bar{\mathbf{\Phi}}\right]^{ij}=\int_{\Gamma_j}\begin{bmatrix}F_{11}^{ij} & F_{12}^{ij}\\ F_{21}^{ij} & F_{22}^{ij}\end{bmatrix}_{o}^{T}\begin{bmatrix}\bar{\phi}_q & 0\\ 0 & \bar{\phi}_q\end{bmatrix}d\Gamma \tag{49}$$

$$\left[\mathbf{F}^{f}\mathbf{M}\right]^{in}=\int_{2\pi}^{0}\begin{bmatrix}\widehat{F}_{11}^{in} & \widehat{F}_{12}^{in}\\ \widehat{F}_{21}^{in} & \widehat{F}_{22}^{in}\end{bmatrix}_{f}^{T}\begin{bmatrix}M_q & 0\\ 0 & M_q\end{bmatrix}R_n d\theta \tag{50}$$

$$\left[\mathbf{G}^{\Theta}\mathbf{M}\right]^{in}=\int_{2\pi}^{0}\begin{bmatrix}\widehat{G}_{11}^{in} & \widehat{G}_{12}^{in}\\ \widehat{G}_{21}^{in} & \widehat{G}_{22}^{in}\end{bmatrix}_{\Theta}^{T}\begin{bmatrix}M_q & 0\\ 0 & M_q\end{bmatrix}R_n d\theta \tag{51}$$

$$\left[\mathbf{F}^{\Theta}\mathbf{M}\right]^{in}=\int_{2\pi}^{0}\begin{bmatrix}\widehat{F}_{11}^{in} & \widehat{F}_{12}^{in}\\ \widehat{F}_{21}^{in} & \widehat{F}_{22}^{in}\end{bmatrix}_{\Theta}^{T}\begin{bmatrix}M_q & 0\\ 0 & M_q\end{bmatrix}R_n d\theta \tag{52}$$

and

$$\begin{cases}\left[\mathbf{F}\bar{\mathbf{\Phi}}\right]^{ij}=\left[\mathbf{F}\bar{\mathbf{\Phi}}\right]^{ij} & \text{if } i\neq j\\ \left[\mathbf{F}\bar{\mathbf{\Phi}}\right]^{ij}=\left[\mathbf{F}\bar{\mathbf{\Phi}}\right]^{ij}+\left[\mathbf{C}\right]^{i} & \text{if } i=j\end{cases} \tag{53}$$

$$\begin{cases}\left[\mathbf{F}^{f}\mathbf{M}\right]^{in}=\left[\mathbf{F}^{f}\mathbf{M}\right]^{in} & \text{if } i\neq n\\ \left[\mathbf{F}^{f}\mathbf{M}\right]^{in}=\left[\mathbf{F}^{f}\mathbf{M}\right]^{in}+\left[\mathbf{C}\right]^{i} & \text{if } i=n\end{cases} \tag{54}$$

$$\begin{cases}\left[\mathbf{F}^{\Theta}\mathbf{M}\right]^{in}=\left[\mathbf{F}^{\Theta}\mathbf{M}\right]^{in} & \text{if } i\neq n\\ \left[\mathbf{F}^{\Theta}\mathbf{M}\right]^{in}=\left[\mathbf{F}^{\Theta}\mathbf{M}\right]^{in}+\left[\mathbf{C}\right]^{i} & \text{if } i=n\end{cases} \tag{55}$$

The boundary integral equation for each inclusion[†]:

$$\mathbf{c}_{ij}^{p}(\xi)u_i(\xi)=\int_0^{2\pi}\left[-\widehat{G}_{ij}^{p}\left(R,\theta,\widehat{\xi}\right)t_i^{f}(\theta)+\widehat{F}_{ij}^{p}\left(R,\theta,\widehat{\xi}\right)u_i^{f}(\theta)\right]Rd\theta \tag{56}$$

is written in the discretized form as:

$$\left[\mathbf{c}^{p}\right]^{i}\{\mathbf{U}\}^{i}=\int_{2\pi}^{0}\left[\mathbf{G}^{p}\right]^{T}[\mathbf{M}]Rd\theta\{\mathbf{T}\}-\int_{2\pi}^{0}\left[\mathbf{F}^{p}\right]^{T}[\mathbf{M}]Rd\theta\{\mathbf{U}\} \tag{57}$$

where $\{\mathbf{U}\}$ and $\{\mathbf{T}\}$ are the displacement and traction column vector for the inclusion. Equation (57) is rewritten as:

$$\left[\mathbf{c}^{p}\right]^{i}\{\mathbf{U}\}^{i}=\sum_{n=1}^{NNP}\left[\int_{2\pi}^{0}\left[\mathbf{G}^{p}\right]^{T}\left[\mathbf{M}_q\right]Rd\theta\{\mathbf{T}\}^{n}\right]-\sum_{n=1}^{NNP}\left[\int_{2\pi}^{0}\left[\mathbf{F}^{p}\right]^{T}\left[\mathbf{M}_q\right]Rd\theta\{\mathbf{U}\}^{n}\right] \tag{58}$$

where $\{\mathbf{U}\}^{n}$ and $\{\mathbf{T}\}^{n}$ are the displacement and traction column vector for the *n*-th node and $\left[\mathbf{M}_q\right]$ is the interpolation function sub-matrix corresponding to the *q*-th node. In a more compact form:

$$\left[\mathbf{c}^{p}\right]^{i}\{\mathbf{U}\}^{i}=\sum_{n=1}^{NNP}\left[\left[\mathbf{G}^{p}\mathbf{M}\right]^{in}\{\mathbf{T}\}^{n}\right]-\sum_{n=1}^{NNP}\left[\left[\mathbf{F}^{p}\mathbf{M}\right]^{in}\{\mathbf{U}\}^{n}\right] \tag{59}$$

with the following definitions:

$$\left[\mathbf{G}^{p}\mathbf{M}\right]^{in}=\int_{2\pi}^{0}\begin{bmatrix}\widehat{G}_{11}^{in} & \widehat{G}_{12}^{in}\\ \widehat{G}_{21}^{in} & \widehat{G}_{22}^{in}\end{bmatrix}_p^{T}\begin{bmatrix}M_q & 0\\ 0 & M_q\end{bmatrix}R_n d\theta \tag{60}$$

$$\left[\mathbf{F}^{p}\mathbf{M}\right]^{in}=\int_{2\pi}^{0}\begin{bmatrix}\widehat{F}_{11}^{in} & \widehat{F}_{12}^{in}\\ \widehat{F}_{21}^{in} & \widehat{F}_{22}^{in}\end{bmatrix}_p^{T}\begin{bmatrix}M_q & 0\\ 0 & M_q\end{bmatrix}R_n d\theta \tag{61}$$

and with:

$$\begin{cases}\left[\mathbf{F}^{p}\mathbf{M}\right]^{ij}=\left[\mathbf{F}^{p}\mathbf{M}\right]^{ij} & \text{if } i\neq j\\ \left[\mathbf{F}^{p}\mathbf{M}\right]^{ij}=\left[\mathbf{F}^{p}\mathbf{M}\right]^{ij}+[\mathbf{c}]^{i} & \text{if } i=j\end{cases} \tag{62}$$

The boundary integral equation for the inclusion domain in the discretized form is written in compact form as:

$$\sum_{n=1}^{NNP}\left[\left[\mathbf{F}^{p}\mathbf{M}\right]^{in}\{\mathbf{U}\}^{n}\right]=\sum_{n=1}^{NNP}\left[\left[\mathbf{G}^{p}\mathbf{M}\right]^{in}\{\mathbf{T}\}^{n}\right] \tag{63}$$

Carrying the collocation process (Brebbia & Dominguez, 1992) over all boundary points, the following system of equations results:

[†] the positive sign in the second term of the RHS is due to considerations on the normal in expressions (5)-(8).

$$\begin{aligned}
\left[\mathbf{F}^{oo}\right]\left\{\mathbf{U}^{o}\right\}+\left[\mathbf{F}^{op}\right]\left\{\mathbf{U}^{p}\right\}+\left[\mathbf{F}^{of}\right]\left\{\mathbf{U}^{f}\right\}&=\left[\mathbf{G}^{oo}\right]\left\{\mathbf{T}^{o}\right\}+\left[\mathbf{G}^{op}\right]\left\{\mathbf{T}^{p}\right\}\\
\left[\mathbf{F}^{po}\right]\left\{\mathbf{U}^{o}\right\}+\left[\mathbf{F}^{pp}\right]\left\{\mathbf{U}^{p}\right\}+\left[\mathbf{F}^{pf}\right]\left\{\mathbf{U}^{f}\right\}&=\left[\mathbf{G}^{po}\right]\left\{\mathbf{T}^{o}\right\}+\left[\mathbf{G}^{pp}\right]\left\{\mathbf{T}^{p}\right\}\\
\left[\mathbf{F}^{fo}\right]\left\{\mathbf{U}^{o}\right\}+\left[\mathbf{F}^{fp}\right]\left\{\mathbf{U}^{p}\right\}+\left[\mathbf{F}^{ff}\right]\left\{\mathbf{U}^{f}\right\}&=\left[\mathbf{G}^{fo}\right]\left\{\mathbf{T}^{o}\right\}+\left[\mathbf{G}^{fp}\right]\left\{\mathbf{T}^{p}\right\}
\end{aligned} \tag{64}$$

for the material matrix and:

$$\left[\mathbf{F}^{pp}\right]\left\{\mathbf{U}^{p}\right\}=\left[\mathbf{G}^{pp}\right]\left\{\mathbf{T}^{p}\right\} \tag{65}$$

for each inclusion, still regarding the interface conditions. In this notation, the first superscript denotes the boundary where the collocation is carried out, and the second denotes the boundary of integration. The global equation system results:

$$\begin{bmatrix}
\mathbf{F}^{oo} & \mathbf{F}^{op} & \mathbf{F}^{of}\\
\mathbf{F}^{po} & \mathbf{F}^{pp} & \mathbf{F}^{pf}\\
\mathbf{F}^{fo} & \mathbf{F}^{fp} & \mathbf{F}^{ff}\\
0 & \mathbf{F}^{pp} & 0
\end{bmatrix}\begin{Bmatrix}\mathbf{U}^{o}\\ \mathbf{U}^{p}\\ \mathbf{U}^{f}\end{Bmatrix}=\begin{bmatrix}
\mathbf{G}^{oo} & \mathbf{G}^{op}\\
\mathbf{G}^{po} & \mathbf{G}^{pp}\\
\mathbf{G}^{fo} & \mathbf{G}^{fp}\\
0 & \mathbf{G}^{pp}
\end{bmatrix}\begin{Bmatrix}\mathbf{T}^{o}\\ \mathbf{T}^{p}\end{Bmatrix} \tag{66}$$

or

$$\left[\mathbf{F}\right]\left\{\mathbf{U}\right\}=\left[\mathbf{G}\right]\left\{\mathbf{T}\right\} \tag{67}$$

where $\left[\mathbf{F}\right]$ and $\left[\mathbf{G}\right]$ are the known coefficient matrices of the boundary element method.

2.4 Numerical evaluation of the coefficient matrix

The accuracy of the BEM for elastostatics is critically dependent on the correct evaluation of the boundary integrals. In this work, the integrals of the hole elements formulation are evaluated numerically using the well known Gauss-Legendre quadrature rules (Stroud & Secrest, 1966):

$$\int_{-1}^{1}\psi\left(x\right)dx=\sum_{i=1}^{n}w_i\psi\left(x_i\right) \tag{68}$$

where $\psi\left(x_i\right)$ is the value of the kernel evaluated on the Gauss's station x_i and w_i are the corresponding weights for the Gauss's points. The use of the equation (68) implies the mapping of the integrals (48)-(52) and (60)-(61) to the normalized space.

The integral (48) contains *weakly singular kernels* and are calculated with the well known co-ordinate transformation proposed by Telles (1987).

The integral (49) contains *strongly singular kernels*, which are calculated in an indirect way by using the *rigid body displacements* technique (Brebbia & Dominguez, 1992). In this case, the singular submatrices of $\mathbf{F}^{oo}$ in equation (66) are evaluated by using:

$$\left[\mathbf{F}\right]^{ii}=-\sum_{j=1}^{NNO+NNF+2NNP}\left[\mathbf{F}\right]^{ij}\quad\text{for } j\neq i \tag{69}$$

It is worth noting that the summation is carried out over the total number of nodes.

The numerical integration of the hole or inclusion matrices (equations (50), (52) and (61)) also deserves special attention, as their kernels are strongly singular. The rigid body displacements technique cannot be used in this case because of its inherent inaccuracy when integrating curvilinear elements (Banerjee, 1994; Guiggiani & Casalini, 1989). In the work of Henry & Banerjee (1991) and Banerjee & Henry (1992) the outer collocation (fictitious domain) to calculate these singular integrals is proposed. In present implementation, the integration of these kernels is accomplished by the direct method. Details on the direct method can be found in the works of Guiggiani et al. (1992), Guiggiani (1998) and Marczak & Creus (2002). The key point in the direct method is to expand asymptotically the kernel singular K_{ij} using Laurent's Series around the image of the load point. The solution of the strongly singular integral is then restated as a regular integral plus one scalar term evaluated on the singular pole. Once the asymptotic expansions $\mathbf{F}_{-1}$ (Marczak & Creus, 2002) are known, standard Gauss-Legendre quadrature suffices to accomplish the numerical evaluation. Buroni (2006) developed the expressions for the Laurent's expansions $\mathbf{F}_{-1}$ that regularize the integrals in the equations (50), (52) and (61):

$$F_{-1}^{12} = -\frac{(1-2\nu)}{4\pi(1-\nu)} M_a(p)$$
$$F_{-1}^{21} = \frac{(1-2\nu)}{4\pi(1-\nu)} M_a(p) \tag{70}$$

where M_a is a shape function corresponding to kernel, and $p = \eta(\xi)$ the image of the load point on the normalized domain η. Details on the direct evaluation of the strongly singular integrals in the hole or inclusion element can be found in the work of Buroni (2006).

2.5 System of equations

Considering the boundary conditions in the linear equations system (67), n_1 values of displacements and n_2 values of tractions are known in the outer material matrix boundaries Γ_1 and Γ_2 ($\Gamma_1 \cup \Gamma_2 = \Gamma_O$), respectively. Now, the quantity of unknowns in the outer material matrix boundary is $n_1 + n_2 = 2NNO$. Thus, the system of equations has $2NNO + 4NNP + 2NNF$ unknowns and $2NNO + 4NNP + 2NNF$ equations. This system can be rearranged in a way that all unknowns are in the same vector. Firstly, considering that the tractions on the inclusion boundary are unknown:

$$\begin{bmatrix} \mathbf{F}^{oo} & \mathbf{F}^{op} & \mathbf{F}^{of} & -\mathbf{G}^{op} \\ \mathbf{F}^{po} & \mathbf{F}^{pp} & \mathbf{F}^{pf} & -\mathbf{G}^{pp} \\ \mathbf{F}^{fo} & \mathbf{F}^{fp} & \mathbf{F}^{ff} & -\mathbf{G}^{fp} \\ 0 & \mathbf{F}^{pp} & 0 & -\mathbf{G}^{pp} \end{bmatrix} \begin{Bmatrix} \mathbf{U}^{o} \\ \mathbf{U}^{p} \\ \mathbf{U}^{f} \\ \mathbf{T}^{p} \end{Bmatrix} = \begin{bmatrix} \mathbf{G}^{oo} \\ \mathbf{G}^{po} \\ \mathbf{G}^{fo} \\ 0 \end{bmatrix} \{\mathbf{T}^{o}\} \tag{71}$$

Then, the boundary conditions can be introduced in equation (71) and the columns in the matrices $\mathbf{F}^{oo}$, $\mathbf{F}^{po}$, $\mathbf{F}^{fo}$, $\mathbf{G}^{oo}$, $\mathbf{G}^{po}$ and $\mathbf{G}^{fo}$ are rearranged so that:

$$\begin{bmatrix} \bar{\mathbf{A}}^{oo} & \mathbf{F}^{op} & \mathbf{F}^{of} & -\mathbf{G}^{op} \\ \bar{\mathbf{A}}^{po} & \mathbf{F}^{pp} & \mathbf{F}^{pf} & -\mathbf{G}^{pp} \\ \bar{\mathbf{A}}^{fo} & \mathbf{F}^{fp} & \mathbf{F}^{ff} & -\mathbf{G}^{fp} \\ 0 & \mathbf{F}^{pp} & 0 & -\mathbf{G}^{pp} \end{bmatrix} \begin{Bmatrix} \mathbf{x}^{o} \\ \mathbf{U}^{p} \\ \mathbf{U}^{f} \\ \mathbf{T}^{p} \end{Bmatrix} = \begin{bmatrix} \bar{\mathbf{B}}^{oo} \\ \bar{\mathbf{B}}^{po} \\ \bar{\mathbf{B}}^{fo} \\ 0 \end{bmatrix} \left\{ \bar{\mathbf{x}}^{o} \right\} \tag{72}$$

This gives final system of equations:

$$\begin{bmatrix} \bar{\mathbf{A}}^{oo} & \mathbf{C} \\ \mathbf{B} & \mathbf{D} \end{bmatrix} \begin{Bmatrix} \mathbf{x}^{o} \\ \mathbf{x}_{a} \end{Bmatrix} = \begin{Bmatrix} \mathbf{b}_{\mathbf{o}} \\ \mathbf{b}_{a} \end{Bmatrix} \tag{73}$$

or

$$\left[\mathbf{A}\right]\left\{\mathbf{x}\right\} = \left\{\mathbf{b}\right\} \tag{74}$$

where the following definitions were used:

$$\left[\mathbf{C}\right] = \begin{bmatrix} \mathbf{F}^{op} & \mathbf{F}^{of} & -\mathbf{G}^{op} \end{bmatrix}, \left[\mathbf{B}\right] = \begin{bmatrix} \bar{\mathbf{A}}^{po} \\ \bar{\mathbf{A}}^{fo} \\ 0 \end{bmatrix}, \left[\mathbf{D}\right] = \begin{bmatrix} \mathbf{F}^{pp} & \mathbf{F}^{pf} & -\mathbf{G}^{pp} \\ \mathbf{F}^{fp} & \mathbf{F}^{ff} & -\mathbf{G}^{fp} \\ \mathbf{F}^{pp} & 0 & -\mathbf{G}^{pp} \end{bmatrix} \tag{75}$$

$$\left\{\mathbf{x}_{a}\right\} = \begin{Bmatrix} \mathbf{U}^{p} \\ \mathbf{U}^{f} \\ \mathbf{T}^{p} \end{Bmatrix}, \left\{\mathbf{b}_{\mathbf{o}}\right\} = \left[\bar{\mathbf{B}}^{oo}\right]\left\{\bar{\mathbf{x}}^{o}\right\}, \left\{\mathbf{b}_{a}\right\} = \begin{bmatrix} \bar{\mathbf{B}}^{po} \\ \bar{\mathbf{B}}^{fo} \\ 0 \end{bmatrix} \left\{\bar{\mathbf{x}}^{o}\right\} \tag{76}$$

In material modeling or in the implementation of the optimization algorithms, where it is necessary solve a BVP in the microstructure (each one with a different distribution of inhomogeneities) many times, the BEM has a special advantage: it is not necessary to recalculate the matrix $\bar{\mathbf{A}}^{oo}$ each time, and it can be stored out-of-core with the obvious savings in computational efficiency. In this case, a *static condensation* in the system of equations (74) is implemented. First, one can solve the displacements and tractions in the boundary of the holes, and the tractions in the boundary of inclusions with:

$$\left[\mathbf{D} - \mathbf{B}\left(\bar{\mathbf{A}}^{oo}\right)^{-1}\mathbf{C}\right]\left\{\mathbf{x}_{a}\right\} = \left\{\mathbf{b}_{a} - \mathbf{B}\left(\bar{\mathbf{A}}^{oo}\right)^{-1}\mathbf{b}_{\mathbf{o}}\right\} \tag{77}$$

and then one can obtain the unknowns in the outer boundary of matrix with the expression:

$$\left\{\mathbf{x}_{\mathbf{o}}\right\} = \left[\left(\bar{\mathbf{A}}^{oo}\right)^{-1}\right]\left\{\mathbf{b}_{\mathbf{o}} - \mathbf{C}\mathbf{x}_{a}\right\} \tag{78}$$

This reduces the computer memory requirements needed, since a smaller system of equations is generated.

3 NUMERICAL APPLICATIONS

In this section, a number of tests solved with the hole element are analyzed to make a preliminary assertion of the quality of the results. In all cases presented herein, the Young modulus is 210 GPa, the Poisson ratio is 0.3 and the plane stress hypothesis is assumed. The

first example consists of a square plate of dimensions l with a cylindrical hole of diameter D at the center (see Fig. 7). The plate is submitted to uniform normal tractions t_1 and is simply supported on the sides CD and DA. The Figs. 8 and 9 show the results of several D/l ratios for 3, 4, 5 and 6 nodes elements compared with results obtained with the hole modeled using 16 discontinuous quadratic elements. In Fig. 8, the ratio between the maximum displacement in the x_1-direction on the side AB calculated with the hole element and calculated with conventional element is plotted. In Fig. 9, the minimum displacement in the x_2-direction on the side BC is considered. These figures reveal the loss of the quality in the results when diameter of the hole becomes close to the plate dimensions. This fact is a consequence of the present implementation taking no special attention with quasi-singular integrals, which becomes more conspicuous when collocation points are close to the hole/inclusion element. It is worth to mention that in numerical experiments ill-conditioned systems resulted for ratios $D/l \geq 0.8$.

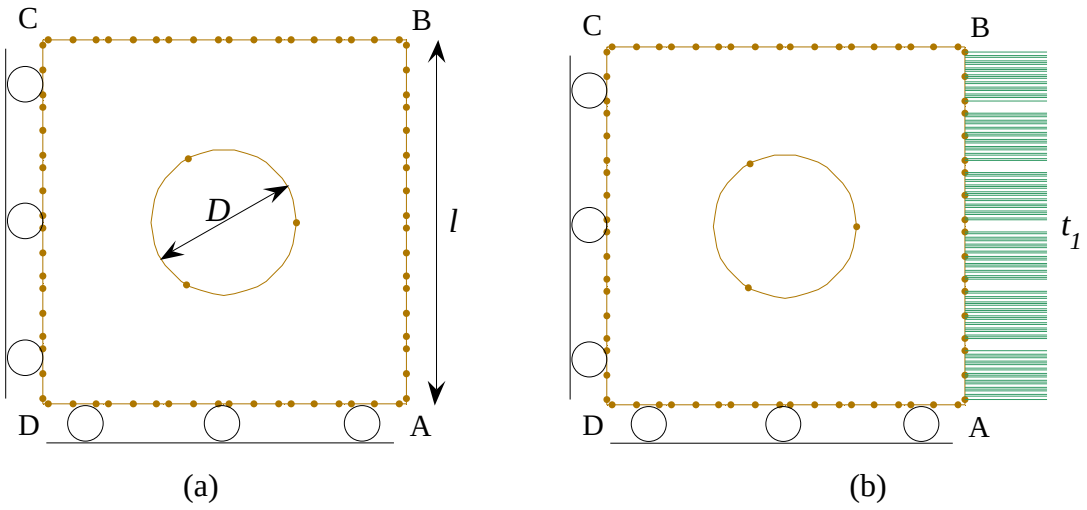

Figure 7: Squared plate a single cylindrical hole.

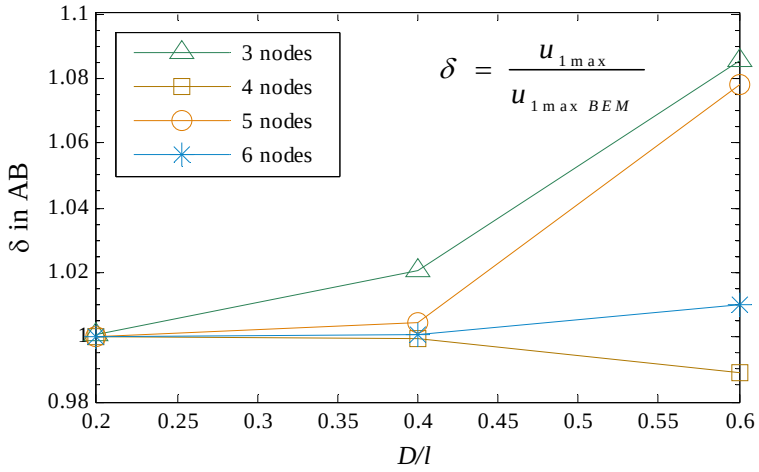

Figure 8: Ratio between the maximum displacement in the x_1-direction on the side AB calculated with the 3, 4, 5 and 6 nodes hole element and that calculated with the hole discretized using 16 quadratic discontinuous elements.

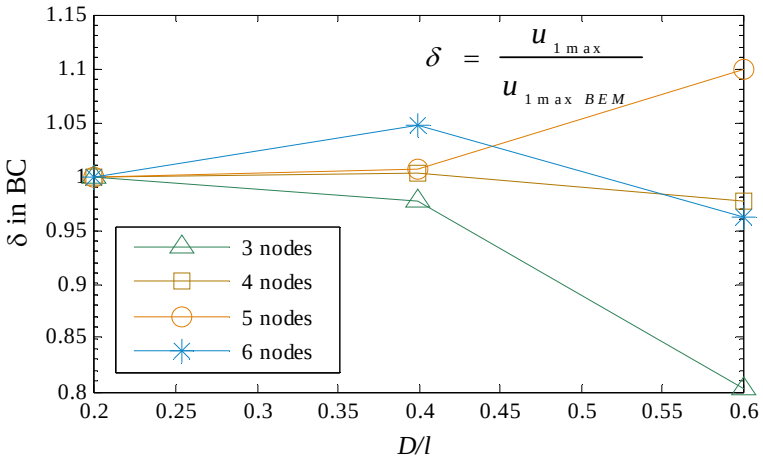

Figure 9: Ratio between the minimum displacement in the x_2-direction on the side BC calculated with the 3, 4, 5 and 6 nodes hole element and that calculated with the hole discretized using 16 quadratic discontinuous elements.

In next example, the interaction between two holes is assessed. A plate similar to the one of the first example is analyzed, but containing two holes as is indicated in Fig. 10. The dimension l of plate is 20mm, the radius is unitary and the distance between hole centers is d (see Fig. 11).

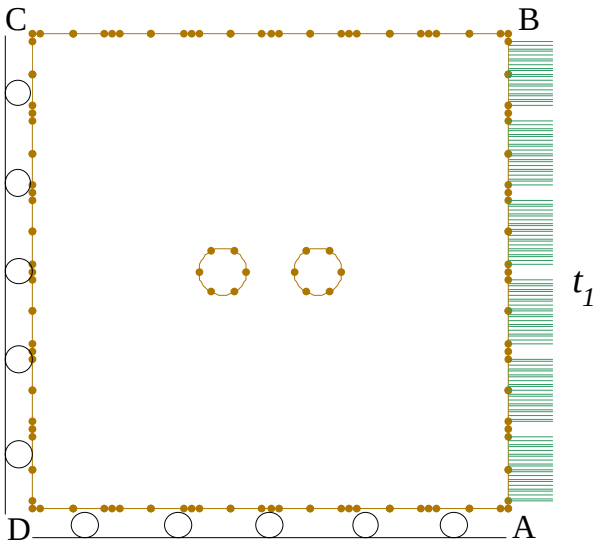

Figure 10: Squared plate with two cylindrical holes.

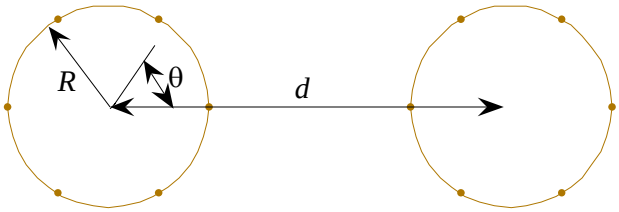

Figure 11: Characteristic parameters for two holes interaction.

Figs. 12 -15 illustrates the displacements of the left hole boundary for ratios *R/d* of 0.25, 0.285, 0.375 and 0.44, respectively.

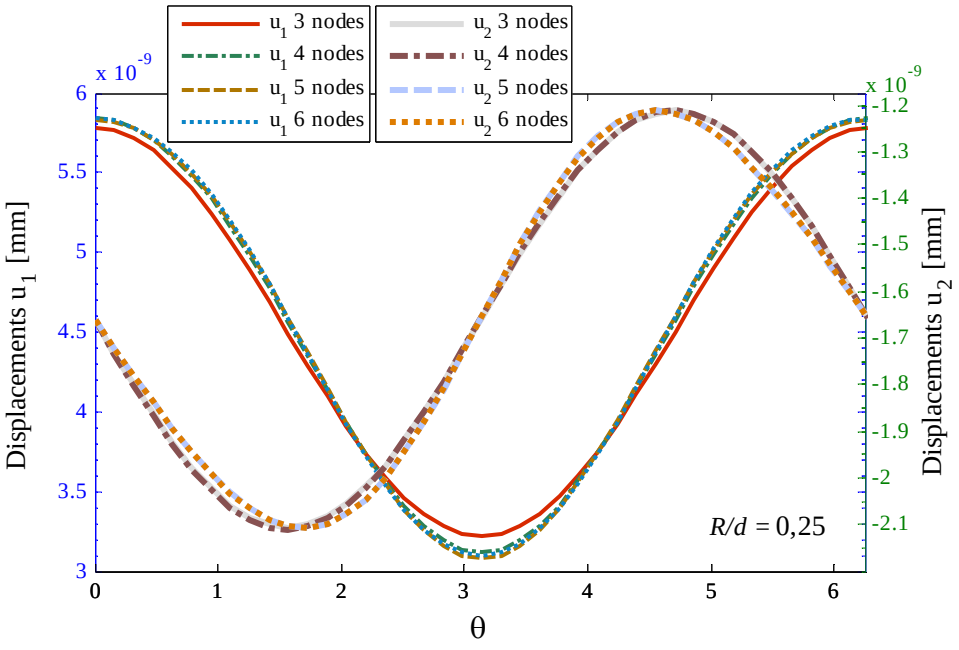

Figure 12: Displacements in the left hole boundary in the case of a plate with two holes. *R/d* = 0.25.

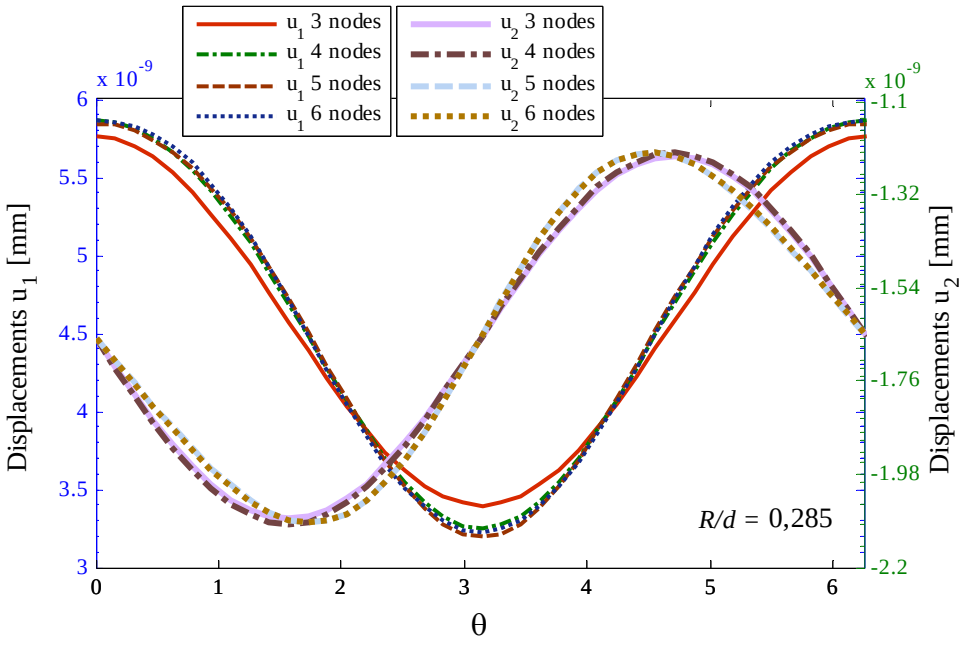

Figure 13: Displacements in the left hole boundary in the case of a plate with two holes. *R/d* = 0.285.

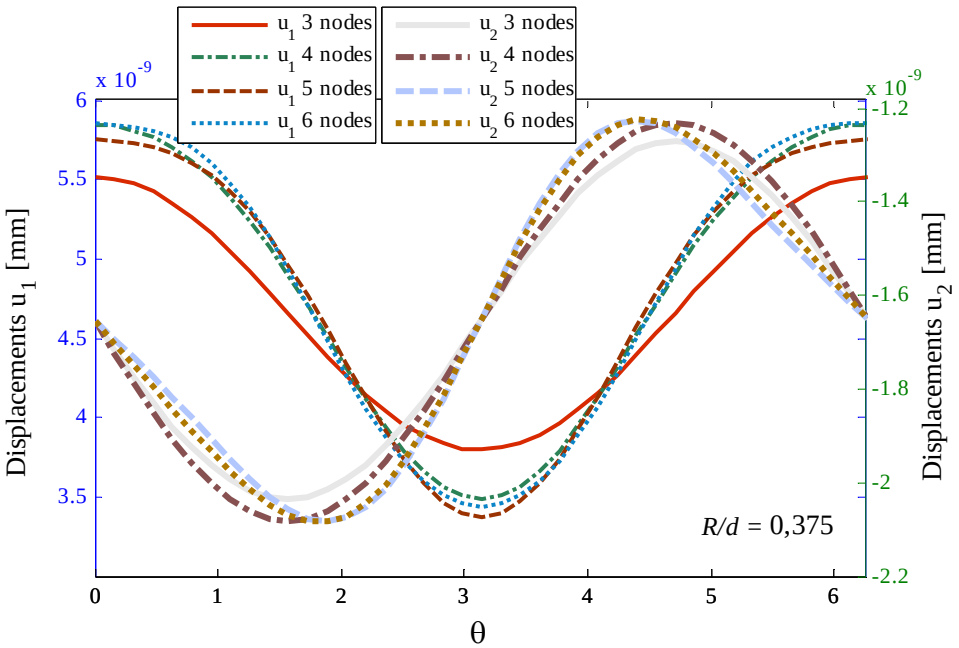

Figure 14: Displacements in the left hole boundary in the case of a plate with two holes. *R/d* = 0.375.

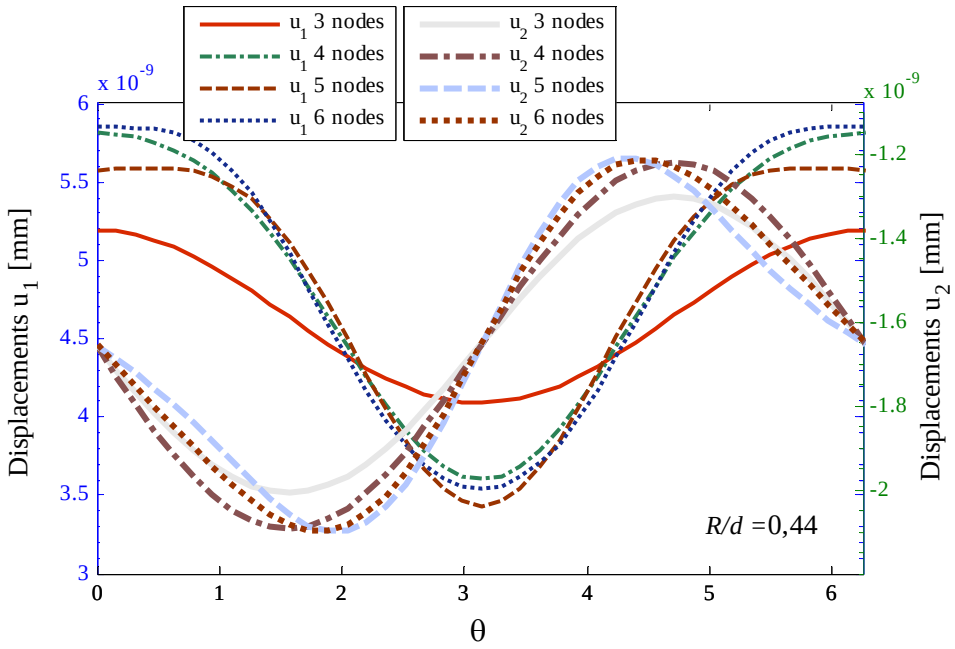

Figure 15: Displacements in the left hole boundary in the case of a plate with two holes. *R/d* = 0.44.

4 CONCLUSIONS

A boundary element formulation for the two-dimensional analysis of microstructures containing randomly distributed cylindrical inhomogeneities has been presented in this paper. The formulation includes a new family of elements such that each void or inclusion is modeled with a single boundary element. Therefore, the amount of data and computational cost is considerably reduced and the microstructure discretization strategy becomes simpler when compared to the conventional BEM or other discretization based methods. The numerical integration of the key terms is accomplished by the direct method, resulting in a regularized element. In addition, a static condensation scheme has been presented to reduce the size of the system of equations, which is especially advisable when solving many times the same problem, but using different inhomogeneities distributions.

The accuracy of the new hole/inclusion elements has been verified through several examples. The proposed approach has shown to be very attractive to simulate the behavior of micro-heterogeneous composite materials containing many voids and inclusions of different sizes. However, no special care was taken so far to integrate quasi-singular integrals arising when two holes/inclusions are very close. As a consequence, when *D*/*l* ratios larger than 80% are analyzed, the system of equations may become ill-conditioned, as indicated by Figs. 8 and 9. As far as the proposed elements are concerned, there is an important improvement in the quality of results with the 4-node element with respect to the 3-node element without meaning a significant increase in the computational cost. Results for the higher order elements are even better, but they increase the computational cost without many improvements on the final results, particularly in problems dealing with a large number of holes/inclusions.

ACKNOWLEDGEMENTS

The first author wishes to express his thanks to CNPq for the financial support and is also grateful to Prof. Adrián P. Cisilino for very useful discussions. This work was partially financed by PROSUL 490185/2005-3 and CAPES/SETCIP 048/03 projects.

REFERENCES

P.K. Banerjee. *The Boundary Element Methods in Engineering*. Mc Graw-Hill Book Company, 1994.

P. K. Banerjee & D.P. Henry. Elastic Analysis of Three-dimensional Solids with Small Holes by BEM, *International Journal of Solids and Structures*, vol. 29, pp. 2423-2440, 1992.

F.C. Buroni. Modelagem e Projeto Computacional de Materiais Micro-Porosos com Distribuição Aleatória Utilizando uma Formulação de Elementos de Contorno. Master thesis, Universidade Federal de Rio Grande do Sul, Porto Alegre, Brazil, 2006.

C.A. Brebbia & J. Dominguez. *Boundary Elements. An Introductory Course*. Second Edition. Computational Mechanics Publications. Southampton Boston – Mc Graw-Hill Book Company, 1992.

M. Guiggiani. *Formulation and Numerical Treatment of Boundary Integral Equations with Hypersingular Kernels*. V. Sladek and J Sladek, eds. Singular Integrals in B. E. Methods, Computational Mechanics Publications, Chapter 3, pp. 85-124, 1998.

M. Guiggiani & P. Casalini. Rigid–body Translation with Curved Boundary Elements. *Applied Mathematical Modeling*. vol. 13, pp. 365-368, 1989.

M. Guiggiani, G. Krishnasamy, T. J. Rudolphi & F. J. Rizzo. A General Algorithm for the Numerical Solution of Hypersingular Boundary Integral Equations. *Journal of Applied Mechanics*, vol. 59, pp. 604-614, 1992.

D.P. Henry & P.K. Banerjee. Elastic Stress Analysis of Three-Dimensional Solids with Small Holes by BEM. *International Journal for Numerical Methods in Engineering*, vol. 31, pp. 369–384, 1991.

R.J. Marczak & G.J. Creus. Direct Evaluation of Singular Integrals in Boundary Element Analysis of Thick Plates. *Engineering Analysis with Boundary Elements*, vol. 26, pp. 653–665, 2002.

J.C.F. Telles. A Self-adaptive Co-ordinate Transformation for Efficient Numerical Evaluation of General Boundary Element Integrals. *International Journal of Numerical Methods in Engineering*. vol. 24, pp. 959-973, 1987.

A.H. Stroud & D. Secrest. *Gaussian Quadrature Formulas*, Prentice-Hall, 1966.

Q-S. Yang & Q-H. Qin. Micro-mechanical Analysis of Composite Materials by BEM. *Engineering Analysis with Boundary Elements*, vol.28, pp. 919-926, 2004